

# Numerical investigation of natural convection heat transfer from horizontal circular cylinder in a vented enclosure filled with nanofluids

Dr. OMAR MOHAMMAD ALI<sup>(1)</sup> BAN AWNI MATLOOB<sup>(2)</sup>

<sup>(1)</sup>Department of Refrigeration and Air Conditioning, Collage of Engineering, Technical Institute of Zakho, Zakho, Kurdistan, Iraq

<sup>(2)</sup>Department of Mechanical, Collage of Engineering, Thermal and Power System, University of Mosul, Iraq

**Abstract:** In this research, the natural convection heat transfer from the horizontal circular cylinder in a vented enclosure filled with nanofluid is investigated numerically. Governing equations settling in the vorticity-stream function formulation is inclusive in the numerical work, which transformed into fitted body coordinate system. The study covered the following ranges of Rayleigh number  $10^4 \leq Ra \leq 10^6$ , nanofluid volume fraction  $0 \leq \phi \leq 0.2$ , enclosure width  $1.667 \leq W/D \leq 5$ , and opening size  $0 \leq O/W \leq 1$ . The effect of Rayleigh number, nanofluid volume fraction, enclosure width, and opening size on the Nusselt number, flow patterns and isotherms were investigated. The result shows that the Nusselt number is proportional with Rayleigh number, opening size and volume fraction of nanofluid and inversely proportional with enclosure width. The isotherms and flow patterns display the temperature and flow behaviors with changing studied variables. The thickness of thermal boundary layer decreases with increasing Rayleigh number for each opening size, enclosure width and nanofluid volume fraction.

**Keywords:** Natural Convection, Circular Cylinder, Vented Enclosure, Nanofluid.

## NOMENCLATURE

code	Definition	Unit
Nu	The average Nusselt number, (h.D/k).	
$d_{ij}$	The expression of Source in equ. (26).	
h	The coefficient of Convective heat transfer	W/m <sup>2</sup> .°C
cp	Specific heat at constant pressure.	KJ/kg.°C
J	Jacobian.	
$K_{nf}$	the nanofluid thermal conductivity .	W/m.°C
P	Coordinate control function.	
Q	Coordinate control function.	
Pr	Prandtl number, (v/α).	
Ra	Rayleigh number	
g	Gravitational acceleration.	m/s <sup>2</sup>
t	Time.	seconds
T	Temperature.	°C
u	Velocity in x-direction.	m/s
v	Velocity in y-direction.	m/s
W	Enclosure Width.	cm
W	Relaxation factor.	
x	Horizontal direction in physical domain.	m

X	Dimensionless horizontal direction in physical domain.	
y	Vertical direction in physical domain.	m
Y	Dimensionless vertical direction in physical domain.	

## Greek Symbols

$\Delta T$	Difference between environmental temperature & cylinder surface temp.	°C
$\phi$	Volume fraction.	
$\mu_{nf}$	Nanofluid viscosity.	kg/m.s
$\beta$	Thermal expansion Coefficient.	1/°C
$\eta$	Vertical direction in computational domain.	
$\xi$	Horizontal direction in computational domain.	in
$\psi$	Stream Function.	1/sec.
$\Psi$	Dimensionless stream function.	
$\omega$	Vorticity.	1/s
$\varpi$	Dimensionless vorticity.	
$\nu$	Kinematic viscosity.	m <sup>2</sup> /s
$\theta$	Dimensionless temperature.	
$\phi$	Dependent variable.	
$\rho_{nf}$	The nanofluid effective density.	Kg/m <sup>3</sup>
$\alpha_{nf}$	Nanofluid Thermal diffusivity.	m <sup>2</sup> /s

## Subscript

S	Cylinder surface.
nf	Nanofluid.
e	Enclosure.
f	Fluid.
s	Solid.
X	Derivative in x-direction.
Y	Derivative in y-direction.
$\xi$	Derivative in $\xi$ -direction.
D	Diameter of Circular cylinder.
$\psi$	Stream function.
T	Temperature.
$\omega$	Vorticity

**I. INTRODUCTION**

There are numerous methods are obtainable to enhance the heat transfer efficiency. One of them is utilizing a fluid substitute the classical fluids like ethylene glycol, water, engine oil and increases the performance of heat transfer called a nanofluid which can be define as a fluid containing particles with nanometer sized and cause an increases in the properties like thermal diffusivity, stability, thermal conductivity, the coefficient of convective heat transfer and viscosity. A brief show of the relevant literature is offered in the following section.

Shu & Zhu [1] studied the natural convection heat transfer in a concentric annulus between a heated inner circular cylinder and a cold outer square cylinder. It is simulated using the differential quadrature (DQ) method. The vorticity stream function formulation is used as the governing equation, and the coordinate transformation technique is introduced in the DQ computation. The transformation coordinate from physical to computational domain is constituted by an analytical term, and all the geometrical parameters can be calculated perfectly. Numerical results for Ra range from  $10^4$  to  $10^6$  and aspect ratios between 1.67 and 5 are presented. It is found that both Ra and aspect ratio are critical to the patterns of thermal fields and flow. The study suggests that a critical aspect ratio may exist at high Rayleigh number to distinguish the flow and thermal patterns.

Ali et. al. [2] investigated experimentally the natural convection heat transfer from horizontal square cylinder in a square vented enclosure. The studied variables range was  $0.25 \leq O/D \leq 4$ ,  $10^7 \leq Ra \leq 6.6 \times 10^7$  and  $2 \leq W/D \leq 4$ . The results showed an Extrusive increase between Nu and Ra. moreover, Nu proportionally increases with the vent opening size at low enclosure widths. Supreme enhancement percentage is higher than 20% for bounded square cylinder, as contrast with unbounded square cylinder. Abu-Nada & Oztab [3] analyzed numerically the effects of inclination angle on fluid flow and natural convection heat transfer in an enclosure filled with Cu-nanofluid. Use finite volume technique to resolve the governing equation. Rayleigh number range between  $10^3 \leq Ra \leq 10^5$  and the inclination angle is changed from 0 to 120. Results presented that, the impact of concentration of the nanoparticles on Nu is much obvious at low volume fraction than at high volume fraction. Inclination angle considers as a control parameter for a nanofluid filled enclosure. At higher Rayleigh numbers, the percentage enhancement of heat transfer decreases by using nanoparticles.

This paper deals with numerical investigation of natural convection heat transfer, from a horizontal circular cylinder, located in a vented enclosure filled with nanofluid. The work discusses the impact of Rayleigh number, nanofluid volume fraction, opening size and enclosure width on flow distributions, temperature distributions and Nusselt number. The study uses various

range of volume fraction of nanoparticles, opening size, Rayleigh numbers and enclosure width.

**II. MATHEMATICAL FORMULATION**

The governing equations for incompressible, steady, two dimensional, laminar flow under the Boussinesq approximation are the recognized Navier-stokes equation. Primal variables are used to write the governing equations and then extended to the stream function-vorticity formulation [4]. The properties of thermophysical are shown in table (1) and with a Boussinesq flow supposed to be constant [5].

**Table 1. Thermophysical properties of nanoparticles and fluid, Hakan et.al [5]**

Physical Properties	Fluid phase (water)	Nanoparticles (Cu)
Cp (J/kg.°K)	4197	385
k (W/m.°K)	0.613	400
$\rho$ (kg/m <sup>3</sup> )	997.1	8933
$\beta \times 10^{-5}$ (m <sup>2</sup> /sec)	21	1.67
$\alpha \times 10^7$ (m <sup>2</sup> /sec)	1.47	1163.1

The governing equation presented as:-

The equation of Continuity:

$$\frac{\partial u}{\partial x} + \frac{\partial v}{\partial y} = 0 \tag{1}$$

The equation of x- momentum:

$$\frac{\partial u}{\partial t} + u \frac{\partial u}{\partial x} + v \frac{\partial u}{\partial y} = - \frac{1}{\rho_{nf}} \frac{\partial p}{\partial x} + v_{nf} \left( \frac{\partial^2 u}{\partial x^2} + \frac{\partial^2 u}{\partial y^2} \right) + g \frac{(\rho\beta)_{nf}}{\rho_{nf}} g \Delta T \tag{2}$$

The equation of y- momentum

$$\frac{\partial v}{\partial t} + u \frac{\partial v}{\partial x} + v \frac{\partial v}{\partial y} = - \frac{1}{\rho_{nf}} \frac{\partial p}{\partial y} + v_{nf} \left( \frac{\partial^2 v}{\partial x^2} + \frac{\partial^2 v}{\partial y^2} \right) + g \frac{(\rho\beta)_{nf}}{\rho_{nf}} g \Delta T \tag{3}$$

The equation of energy

$$\frac{\partial T}{\partial t} + u \frac{\partial T}{\partial x} + v \frac{\partial T}{\partial y} = \alpha_{nf} \left( \frac{\partial^2 T}{\partial x^2} + \frac{\partial^2 T}{\partial y^2} \right) \tag{4}$$

With Boussinesq approximations, the density is constant for all terms of governing equations, except for the bouncy force term, which density is a linear function of the temperature.

$$\rho = \rho_o(1 - \beta \Delta T) \quad (5)$$

$\beta$  is the thermal expansion coefficient [6].

By used stream function-vorticity formulation, the number of the equations can be reduced.

The stream function ( $\psi$ ) may be offered as

$$u = \frac{\partial \psi}{\partial y}, \quad v = -\frac{\partial \psi}{\partial x} \quad (6)$$

And the vorticity as

$$\omega = \frac{\partial v}{\partial x} - \frac{\partial u}{\partial y} \quad (7)$$

The governing equations in term of the stream function – vorticity formulation become:

Continuity Equation

$$\frac{\partial^2 \Psi}{\partial X^2} + \frac{\partial^2 \Psi}{\partial Y^2} = -\omega \quad (8)$$

Momentum Equation:

$$\frac{\partial \omega}{\partial t} + \frac{\partial \Psi}{\partial Y} \frac{\partial \omega}{\partial X} - \frac{\partial \Psi}{\partial X} \frac{\partial \omega}{\partial Y} = \left[ \frac{\text{Pr}}{(1 - \varphi)^{0.25} \left( (1 - \varphi) + \varphi \frac{\rho_s}{\rho_f} \right)} \left( \frac{\partial^2 \omega}{\partial X^2} + \frac{\partial^2 \omega}{\partial Y^2} \right) + Ra \text{Pr} \left[ \frac{1}{\frac{(1 - \varphi) \rho_f}{\varphi \rho_s} + 1} \frac{\beta_s}{\beta_f} + \frac{1}{\frac{\varphi \rho_f}{(1 - \varphi) \rho_s} + 1} \right] \right] \frac{\partial \theta}{\partial X} \quad (9)$$

Energy Equation

$$\frac{\partial \theta}{\partial t} + \frac{\partial \Psi}{\partial Y} \frac{\partial \theta}{\partial X} - \frac{\partial \Psi}{\partial X} \frac{\partial \theta}{\partial Y} = \frac{\partial}{\partial X} \left( \lambda \frac{\partial \theta}{\partial X} \right) + \frac{\partial}{\partial Y} \left( \lambda \frac{\partial \theta}{\partial Y} \right) \quad (10)$$

Where: 
$$\lambda = \frac{k_{nf}}{(1 - \varphi) + \varphi \frac{(\rho c_p)_s}{(\rho c_p)_f}} \quad (11)$$

The nanofluid thermal diffusivity is [7]:

$$\alpha_{nf} = \frac{k_{nf}}{(\rho c_p)_{nf}} \quad (12)$$

The nanofluid effective density is:

$$\rho_{nf} = ((1 - \varphi)\rho_f + \varphi\rho_s) \quad (13)$$

The nanofluid heat capacitance is:

$$(\rho c_p)_{nf} = ((1 - \varphi)(\rho c_p)_f + \varphi(\rho c_p)_s) \quad (14)$$

The ratio of nanofluids thermal conductivity is for nanoparticles with spherical shape and approximated by the Maxwell–Garnetts model [8]

$$\frac{k_{nf}}{k_f} = \frac{k_s + 2k_f - 2\varphi(k_f - k_s)}{k_s + 2k_f + \varphi(k_f - k_s)} \quad (15)$$

The nanofluid viscosity can be considered as viscosity of a base fluid hold a dilute suspension of tiny rigid spherical particles and it is given by [9].

$$\mu_{nf} = \frac{\mu_f}{(1 - \varphi)^{2.5}} \quad (16)$$

The variables are non-dimensionalized by defining the subsequent parameters [10]:

$$X = \frac{x}{D} \quad Y = \frac{y}{D} \quad U = \frac{uD}{g} \quad V = \frac{vD}{g} \\ \tau = \frac{tg}{D^2} \quad \Psi = \frac{\psi}{g} \quad \omega = \frac{\omega D^2}{g} \quad \theta = \frac{T - T_\infty}{T_c - T_\infty} \quad (17)$$

Employing these non-dimensionalized variables, the governing equations (8)-(10) transformed to this generic shape in the computational space:

$$a_\phi \left\{ \frac{\partial \phi}{\partial t} + \frac{1}{J} \left[ \left( \frac{\partial \psi}{\partial \eta} \phi \right)_\xi - \left( \frac{\partial \psi}{\partial \xi} \phi \right)_\eta \right] \right\} = \nabla(b_\phi \nabla \phi) + d_\phi \quad (18)$$

Where  $\frac{\partial \phi}{\partial t}$  is the expression of unsteady?

$\frac{1}{J} \left[ \left( \frac{\partial \psi}{\partial \eta} \phi \right)_\xi - \left( \frac{\partial \psi}{\partial \xi} \phi \right)_\eta \right]$  Is the expression of convective?

$\nabla(b_\phi \nabla \phi)$  Is the expression of diffusion?

$d_\phi$  is the expression of source.

The expression of diffusion in equation (18) is:

$$\nabla(b_\phi \nabla \phi) = \frac{1}{J^2} \left\{ \begin{aligned} &\gamma \frac{\partial}{\partial \xi} \left( b_\phi \frac{\partial \phi}{\partial \xi} \right) - \beta \frac{\partial}{\partial \xi} \left( b_\phi \frac{\partial \phi}{\partial \eta} \right) - \\ &\beta \frac{\partial}{\partial \eta} \left( b_\phi \frac{\partial \phi}{\partial \xi} \right) + \alpha \frac{\partial}{\partial \eta} \left( b_\phi \frac{\partial \phi}{\partial \eta} \right) \end{aligned} \right\} + b_\phi \left[ \sigma \frac{\partial \phi}{\partial \eta} + \tau \frac{\partial \phi}{\partial \xi} \right] \quad (19)$$

Where  $\sigma = \frac{\partial^2 \xi}{\partial x^2} + \frac{\partial^2 \xi}{\partial y^2}$  and  $\tau = \frac{\partial^2 \eta}{\partial x^2} + \frac{\partial^2 \eta}{\partial y^2}$

Changing the dependent variable  $\phi$  to get the governing equations as table (2) [11].

**GRID GENERATION**

Geometric data of the Cartesian coordinates can be formed using algebraic methods, which is used to produce an initial computational grid points. The equations of elliptic partial differential that used are Poisson equations:

$$\xi_{xx} + \xi_{yy} = P(\xi, \eta) \quad (20a)$$

$$\eta_{xx} + \eta_{yy} = Q(\xi, \eta) \quad (20b)$$

Transforming above equations in computational space yields a set of two elliptical PDEs of the form [12]:

$$\alpha x_{\xi\xi} - 2\beta x_{\xi\eta} + \gamma x_{\eta\eta} + J^2(P x_\xi + Q x_\eta) = 0 \quad (21a)$$

$$\alpha y_{\xi\xi} - 2\beta y_{\xi\eta} + \gamma y_{\eta\eta} + J^2(P y_\xi + Q y_\eta) = 0 \quad (21b)$$

Where

$$\alpha = x_\eta^2 + y_\eta^2; \quad \beta = x_\xi x_\eta + y_\xi y_\eta;$$

$$\gamma = x_\xi^2 + y_\xi^2$$

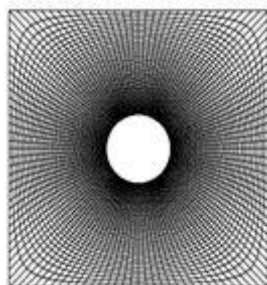


**Fig 1. Transformations of the physical domains into computational domains using elliptic grid generations**

The coordinate control functions P and Q could be selected to impact the grid of structure, [13]. The method of Successive over Relaxation (SOR) is used to acquire the solutions of Poisson and Laplace equation. The relaxation factor is equal to 1.4. The transformation of the

physical domains into computational domains utilizing elliptic grid generation is illustrated in figure (1) [10].

**III. METHOD OF SOLUTION**

The hybrid difference scheme is a combination of central and upwind difference scheme. It makes use of the central difference scheme, which is second order accurate for small pecllet numbers. It turns to upwind difference scheme when central difference scheme produces inaccurate results for high pecllet numbers [14]. The general discretization equation becomes:

$$a_p \phi_p = a_E \phi_E + a_W \phi_W + a_N \phi_N + a_S \phi_S + a_p^o \phi_p^o + a_M \left( \begin{aligned} &\phi_{i+1,j+1} - \phi_{i-1,j-1} \\ &-\phi_{i+1,j-1} + \phi_{i-1,j+1} \end{aligned} \right) + d_{i,j} \dots (22)$$

Where

$$a_M = \frac{\beta b_\phi}{2J^2} \quad (23)$$

$$a_{p^o} = \frac{1}{\Delta t} \quad (24)$$

$$a_p = a_E + a_W + a_N + a_S + a_p^o \quad (25)$$

$$d_{i,j} = \left\{ \begin{aligned} &\omega_{i,j} \quad \text{for } \psi \text{ equation} \\ &0 \quad \text{for temp. equation} \\ &\frac{Ra Pr ff}{8J} \left\{ \begin{aligned} &\theta_{i+1,j} \left( \begin{aligned} &y_{i+1,j+1} - y_{i+1,j-1} \end{aligned} \right) + \\ &\theta_{i,j-1} \left( \begin{aligned} &y_{i+1,j-1} - y_{i-1,j-1} \end{aligned} \right) - \\ &\theta_{i-1,j} \left( \begin{aligned} &y_{i-1,j+1} - y_{i-1,j-1} \end{aligned} \right) - \\ &\theta_{i,j+1} \left( \begin{aligned} &y_{i+1,j+1} - y_{i-1,j+1} \end{aligned} \right) + \\ &y_{i+1,j} - y_{i-1,j} \end{aligned} \right\} \end{aligned} \right. \quad \text{for vorticity equation} \dots (26)$$

Where  $a_W, a_E, a_S, a_N, a_M, a_p^o$  are coefficients of the discretization equation [10].

Using the method of alternating direction (ADI), the resulting algebraic equation is settled in two sweeps. In the premier sweep, the equations are solved implicitly in  $\xi$ -direction and explicitly in  $\eta$ -direction. The implicit discretization equation in  $\xi$ -direction is solved by using Cyclic TriDiagonal Matrix Algorithm (CTDMA) because of its cyclic boundary conditions. On the other sweep, the equations are solved implicitly in  $\eta$ -direction and explicit in  $\xi$ -direction. The implicit discretization equation in  $\eta$ -direction is solved by using TriDiagonal Matrix

Algorithm (TDMA) [6]. The initial conditions of the flux between vented enclosure and heated cylinder are:

$$\left. \begin{aligned} \psi &= 0, \\ \theta &= 0, \\ \omega &= 0. \end{aligned} \right\} \text{ For } t = 0 \quad (27)$$

At the cylinder surface assume constant temperature and for the vorticity this equation is applied

$$\varpi = \frac{2\gamma}{J^2} (\psi_{i,1} - \psi_{i,2}) \quad (28)$$

The enclosure wall is considered as adiabatic surface (no heat transfer)

$$\theta = 0 \quad (29)$$

And for vorticity this equation is applied:

$$\varpi = \frac{2\gamma}{J^2} (\psi_{i,m} - \psi_{i,m-1}) \quad (30)$$

At the lower vent, temperature is supposed equal to free stream flow temperature and the flow assumed as uniform so

$$\varpi = 0 \quad (31)$$

The local heat transfer along the upper opening was equal to the local heat transfer at just point downstream of it:

$$\left. \frac{\partial \theta}{\partial \eta} \right|_m = 0 \quad (32)$$

and for the vorticity

$$\varpi = \frac{2\gamma}{J^2} (\psi_{i,m} - \psi_{i,m-1}) + \frac{1}{J^2} \left( 2\beta \frac{\partial^2 \psi}{\partial \eta \partial \xi} - \tau \frac{\partial \psi}{\partial \xi} - \frac{\partial \psi}{\partial \xi} (2\gamma + \sigma) - \alpha \frac{\partial^2 \psi}{\partial \xi^2} \right) \quad (33)$$

Employing this equation by used backward finite difference method for first and second derivative. The stream function for the enclosure is supposed as constant. While for the cylinder which is a solid surface is supposed as zero because nothing enters into it or leaves from it. For calculation Nusselt number which is used in the determination of heat transfer coefficient entailed the next steps:

$$Nu = \frac{hD}{k_f} \quad (34)$$

The coefficient of heat transfer is:

$$h = \frac{q_w}{T_H - T_l} \quad (35)$$

The thermal conductivity is:

$$k_{nf} = -\frac{q_w}{\partial \theta / \partial n} \quad (36)$$

$$\text{Nusselt number is written as: } Nu = -\frac{k_{nf}}{k_f} \int_0^{2\pi} \frac{\partial \theta}{\partial n} \partial \zeta \quad (37)$$

(37)

The derivative of the non\_ dimensional temperature is calculated utilizing the next form,[4]:

$$\left. \frac{\partial \theta}{\partial n} \right|_{\eta=const.} = \frac{1}{J\sqrt{\gamma}} (-\beta\theta_\xi + \gamma\theta_\eta) = \frac{\sqrt{\gamma}}{J} \frac{\partial \theta}{\partial \eta} \quad \dots (38)$$

$\theta_\xi = 0$  at cylinder surface.

The mass flow rate flowing in and out through lower and upper opening is because the density variance, and it is

$$\text{represented as: } \dot{m} = \sum \rho_{i,m} \frac{u_{i,m} + u_{i+1,m}}{2} \Delta x \Big|_{\eta=m} \quad (39)$$

(39)

Where:

$\rho_{i,m} = \rho_{nf} = ((1-\phi)\rho_f + \phi\rho_s)$  at the lower vent and the upper vent.

The numerical algorithm run by a computer program in (Fortran 90), that is generic for a natural convection from heated cylinder located in a vented enclosure.

#### IV. STABILITY AND GRID INDEPENDENCY TEST

A stability investigation of the numerical method is made for the state  $Ra=10^5$ ,  $W/D=1.667$ ,  $O/W=0.5$ ,  $\phi=0.05$  and  $Pr=0.7$ . Three time steps are chosen with value  $1 \times 10^{-6}$ ,  $5 \times 10^{-6}$ ,  $5 \times 10^{-7}$ . The highest difference between Nu values with various time steps is 3%.

A wide mesh testing procedure was carried to guarantee a grid independent solution. Different mesh combinations were used for the state of  $W/D=2.5$ ,  $Ra=10^4$  and  $10^5$ ,  $Pr=6.2$ . For the present simulation, three grid sizes of  $96 \times 25$ ,  $128 \times 45$  and  $192 \times 50$  are chosen to test the independency of the results with the grid variation. It is observed that the total number of grid points is 2425, 5805 and 9650 respectively. The present code was tested for grid independence by calculating the average Nusselt number. Numerical experiments showed that when the mesh size is above  $96 \times 45$ , the computed Nu remain the same. However for the rest of the calculation in this study choose a grid size of  $128 \times 45$  for better accuracy.

#### VALIDATION TEST

The code validation is an important part for numerical work. A Fortran 90 control volume finite element method code is used in this paper. The code was validated against

the problem of natural convection heat transfer between a heated horizontal cylinder placed concentrically inside a square enclosure by Moukalled & Acharya [15]. To test the code validation, the natural convection problem for high temperature inner circular cylinder and a low temperature outer vented enclosure was tested. The average Nusselt number and maximum stream function for the test case and the work of Moukalled and Acharya are compared in table (3), for  $Pr=0.7$ , various values of  $W/D=1.667, 2.5$  and  $5$  with  $Ra=104$  and  $105$ ,  $O/W=0$  and volume fraction of nanofluid  $\phi=0$ . From table (3) it is clear that the present conclusions are in perfect agreement with those of Moukalled and Acharya.

## V. RESULTS AND DISCUSSION

The numerical result are given for  $Ra=10^4, 10^5$  and  $10^6$  and nanoparticles volume fraction for copper (Cu) based nanofluids which are  $\phi=0, 0.05, 0.1, 0.15, 0.2$ . Water is the base fluid which means the prandtl number equal  $6.2$ . The enclosure width  $W/D=1.667, 2.5$  and  $5$  and opening size  $O/W=0, 0.2, 0.5, 0.8, 1$ . The results obtained are researched under various combinations of relevant parameters involved in the study.

### FLOW PATTERNS AND ISOTHERMS

At  $Ra=104$ , the maximum stream function value varies proportionally with volume fraction of nanofluid. Two identical eddies clarify on two sides of the enclosure wall. Eddies growth linearly below the heat source for all nanoparticles volume fraction. The flow is uniform about the vertical line through the center of the circular cylinder. At pure fluid  $\phi=0$ , the flow is weak, the maximum value of stream function  $\psi_{max}=0.3435332$ . The densely packed of the flow pattern is small. An increase in volume fraction of nanofluid, the maximum stream function value increases slightly with small value. At volume fraction of nanofluid  $\phi=0.1$ ,  $\psi_{max}=0.6175973$ . The densely packed of the flow pattern increase. At  $\phi=0.2$ , the flow is stronger. The value of maximum stream function becomes  $\psi_{max}=0.8591641$ .

However, for  $Ra=10^5$ , the strength of the flow increases and the maximum stream function value enhances. Eddies shape is not uniform. The flow is symmetrical about the vertical line of the circular cylinder. The maximum stream function value change between  $\psi_{max}=4.981700$  at  $\phi=0$  to  $\psi_{max}=13.456240$  at  $\phi=0.2$ . As it can be seen at nanoparticles volume fraction  $\phi=0$  the densely packed of the flow pattern is small. Maximum stream function value increases with increasing the volume fraction of nanofluid. At  $\phi=0.05$  the maximum stream function value  $\psi_{max}=7.196921$ . The densely packed of the flow pattern is high. Four small eddies appear in two sides. At  $\phi=0.2$  the flow is stronger. The densely packed of flow is high. Two eddies appear on the sides of enclosure wall, one longitudinal and one small.

At high Rayleigh number  $Ra=10^6$ , for all volume fraction of nanofluid, the densely packed of the flow is high. The streamlines move up along the inner heat source. The flow is strong and two small eddies appear on both sides of the enclosure wall. The streamlines are closer to cylinder wall. The value of maximum stream function increases with remarkable value by increasing the nanoparticles volume fraction. The maximum value of stream function varies between  $\psi_{max}=38.470870$  at  $\phi=0$  and  $\psi_{max}=79.035880$  at  $\phi=0.2$ .

## VI. CONCLUSION

Natural convection heat transfer from horizontal circular cylinder in a vented enclosure containing nanofluid was investigated numerically for a wide range of Rayleigh number with taking the effect of opening size and enclosure width.

The main conclusions of this paper are:

1. The average Nu increase with increasing the Rayleigh number for each enclosure width, opening size and nanofluid volume fraction.
2. The average Nu increase with increasing opening size for each Rayleigh number, enclosure width and nanofluid volume fraction.
3. The average Nu decrease with increasing enclosure width for each Rayleigh number, opening size and nanofluid volume fraction.
4. The average Nusselt number increase with increasing nanofluid volume fraction for each Rayleigh number, opening size and enclosure width.
5. The strength of the flow increase with increasing the nanofluid volume fraction for each Rayleigh number, opening size and enclosure width.
6. The thickness of thermal boundary layer decrease with increasing the Rayleigh number for each opening size, enclosure width and nanofluid volume fraction
7. The maximum Nusselt number at opening size  $O/W=1$ ,  $W/D=1.667$ ,  $\phi=0.2$  and  $Ra=10^6$  for all parameters.
8. The conduction heat transfer is the dominant mode for low Rayleigh numbers and convection heat transfer is the dominant mode for high Rayleigh numbers.

## REFERENCES

- [1] Shu C., Zhu Y. D., (2002), "Efficient computation of natural convection in a concentric annulus between an outer square cylinder and an inner circular cylinder", International journal for numerical method in fluids, 38:429-445.
- [2] Ali O. M., Kahwaji G. Y., Hussein A. S., (2012), "Experimental investigation of natural convection heat transfer from square cross section cylinder in a vented enclosure", Applied mechanics and materials, 110-116:4451-4464.
- [3] Abo-Nada E., Oztop H. F., (2009), "Effect of inclination angle on natural convection in enclosure filled with Cu-water nanofluid", International journal of heat and fluid flow, 30(4):669-678.

- [4] Fletcher C., A., J., (1988), "Computational Techniques for Fluid Dynamics 2", Springer – Verlag.
- [5] Hakan F. Oztop, Eiyad Abu-Nada, (2008), "Numerical study of natural convection in partially heated rectangular enclosures filled with nanofluids," International Journal of Heat and Fluid Flow 29:1326–1336.
- [6] Ali O. M., kahwaji G. Y., (2014), "Numerical investigation of natural convection heat transfer from circular cylinder inside an enclosure using different types of nanofluid", Journal impact factor, 5(5):214-236.
- [7] Salman A. M., (2011), "An investigation of natural convection heat transfer in a square enclosure filled with nanofluid", Eng. & Technology, 29(12):2346-2363.
- [8] Saleh H., Roslan R., Hashim I., (2011), "Natural convection heat transfer in a nanofluid -filled trapezoidal enclosure", International journal of heat and mass transfer, 54:194-201.
- [9] Brinkman H. C., (1952), "The viscosity of concentrated suspensions and solution", J. Chem. Phys., 20:571-581.
- [10] Ali O. M., (2007), "Experimental and Numerical Investigation of Natural Convection Heat Transfer from Different Cross Section Cylinders in a Vented Enclosure", Ph. D. Thesis, Thermal Power, Mechanical Engineering, University of Mosul.
- [11] Ali O. M., Zaidky R. H. S., Saleem A. M., (2014), "Numerical investigation of natural convection heat transfer from circular cylinder inside an enclosure containing nanofluid", Journal impact factor, 5(12):66-85.
- [12] Pletcher R. H., Tannehill J. C., Anderson D. A., (2013), "computational fluid mechanics and heat transfer", Third edition by Taylor & Francis Group, LLC.
- [13] Thomas P. D., Middle off J. F., (1980), "Direct Control of the Grid Point Distribution in Meshes Generated by Elliptic Equations", AIAA Journal, 18(6): 652-656.
- [14] Spalding D.B., (1972), "A Novel Finite-difference Formulation for Differential Expression Involving Both First and Second Derivatives", Int. J. Numer. Methods Eng., 4:551-559.
- [15] Moukalled F., Acharya S., (1996), "Natural convection in the annulus between concentric horizontal circular and square cylinders", Journal of Thermo physics and Heat Transfer, 10(3):524 –531.